UNIVERSITY OF PARDUBICE

FACULTY OF CHEMICAL TECHNOLOGY

Institute of Environmental and Chemical Engineering

Ing. Abraham Kabutey

Environmental Aspects of Selected Electrochemical and Agglomeration Interactions in Solutions

Theses of the Doctoral Dissertation

Pardubice 2018

Study program: **Chemical and Process Engineering**

Study field: **Environmental Engineering**

Author: **Ing. Abraham Kabutey**

Supervisor: **Assoc. Prof. Dr. Ing. Ladislav Novotný, Dr.Sc.**

Year of the defence: 2018

Reference

KABUTEY, Abraham. *Environmental Aspects of Selected Electrochemical and Agglomeration Interactions in Solutions*. Pardubice, 2018. 80 pages. Doctoral Dissertation (PhD.). University of Pardubice, Faculty of Chemical Technology, Institute of Environmental and Chemical Engineering. Supervisor Assoc. Prof. Dr. Ing. Ladislav Novotný, Dr.Sc.

Annotation

The first section of the work focused on further use, testing and new applications of the recently proposed new possibilities of preparation, arrangement and utilization of potentiometric interactions of amalgam electrodes, especially testing changes of potential responses of silver amalgam electrodes within the ion-exchange treatment of water as well as utilization of potentiometric signal of the zinc amalgam electrode for the detection of concentration changes of zinc sulphate. The second part of the work aimed attention at the special use or testing of the recently described (Novotny) relations for fitting or evaluating adsorption, electrosorption and agglomeration data. In view of this, the fitting kinetics of silver nanoparticles agglomeration in relation to time was described using appropriate statistical methods like the forward stepwise regression analysis.

Anotace

První část práce byla zaměřena na využití, testování a nové aplikace nedávno navržených nových možností přípravy, uspořádání a využití potenciometrických interakcí amalgámových elektrod, zejména na testování změn potenciálové odezvy stříbrných amalgámových elektrod během iontoměničové úpravy vody a dále na využití potenciometrického signálu zinkové amalgámové elektrody pro detekci koncentračních změn roztoků síranu zinečnatého. Druhá část práce byla věnována speciálnímu užití nebo testování nedávno popsaných (Novotného) vztahů, například pro prokládání nebo vyhodnocování adsorpčních, elektrosorpčních a aglomeračních dat. Tímto způsobem bylo provedeno prokládání kinetiky časově závislé aglomerace

nanočástic stříbra, přičemž byly použity statistické metody jako například tzv. postupná regresní analýza.

Keywords

water treatment, ion exchangers, potentiometry, amalgam electrodes, nanoparticles, agglomeration

Klíčová slova

úprava vody, iontoměniče, potenciometrie, amalgámové elektrody, nanočástice, aglomerace

TABLE OF CONTENTS

1. INTRODUCTION

Mutual interactions between different objects are part of the events occurring in the environment and living organisms. These interactions form the natural basis of the various detection, analytical or diagnostic methods and methods of preparation of substances or technological processes. Electrochemical methods or methods of preparation, study and application of systems using particle agglomerates are also part of these processes. Recently, nanochemistry has grown tremendously contributing to the understanding of the heterogeneous processes involving atomic and molecular structures or aggregates that may be desirable or undesirable from an environmental and health point of view. Electrochemistry significantly contributes[1-10] to electro-separation (electro-analytical, -deposition, -coagulation, -degradation) and other processes, purification processes of waters and aqueous solutions, etc., on the accompanying or separate applications of electro-analysis, -indication, -detection, -diagnostics, -signaling, etc. It is also used as a component or in combination with other methods such as filtration, nanofiltration, osmosis, chromatographic detection, optical and other techniques.

The objectives of the work, associated with environmental and health protection, comprised of two sections. The first section focused on further use, testing and new applications of the recently[11-14] proposed new possibilities[12-18,19-21,25] of preparation, arrangement and utilization of amalgam electrodes, their multicomponent potentiometric interactions (influenced by interfacial or limited amperometric processes). As a result of this, testing changes of potential responses of silver amalgam electrode (AgAE) within the ion-exchange treatment of water (after its technological pre-treatment) as well as utilization of potentiometric signal of the zinc amalgam electrode (ZnAE) for the detection of concentration changes of zinc sulphate by nanofiltration were investigated, using the potentiometric arrangements applicable under common operating conditions. The second part of the work aimed attention at the special use or testing of the recently described (Novotny) relations[4,9,10,22-24] for fitting or evaluating adsorption, electrosorption and agglomeration data. In view of this, the fitting kinetics of silver nanoparticles (nAg) agglomeration with time

(based on some similarities with fitting electrosorption data of sodium thiosulphate) was described using appropriate statistical methods like the stepwise regression analysis.

2. EXPERIMENTAL

2.1 Assemblable arrangement for potentiometric measurements with amalgam electrodes and for interfacial or selected additional measurements

2.1.1 Measurements using silver and silver amalgam electrodes for ion exchange water treatment

Prior to the measurement, the entire potentiometric arrangement was tested using a glass ion-selective pH electrode combined with a reference chloride electrode immersed in pH-buffered standard solutions (Electrochemical detectors, s.r.o., Turnov, Czech Republic). Potentiometric measurements were carried out in a circuit made of a specific silver or silver amalgam electrode, reference Ag/AgCl (3 M KCl) with a salt bridge of 0.1 M KNO_3 (Electrochemical detectors, s.r.o., Turnov, Czech Republic) and BM 551 voltmeter (Laboratory devices, Prague, Czech Republic) with the potentiometric module attached, as shown in the studies of[8,18]. The electrodes were inserted into a rack and a computer receptacle Eco-Tribo Polarograph (Eco-Trend Plus s.r.o., Prague, Czech Republic) in a report according to the authors[26-28]. The specific silver electrode (SE) was in the form of a disk of approximately 0.6 mm diameter, which was created by grinding silver wire in a plastic wrap. It was polished with an aluminium emulsion of 0.3 μm (Electrochemical Detectors, s.r.o., Turnov, Czech Republic). Solid silver amalgam electrode (AgAE) in a plastic tip from micropipettes, "Plastic tip"[15,29] (similar to the former "plastic tip" of mercury[34]) or PT-AgE was prepared[15,16,29,30] after filling the silver powder with a particle size of 2 μm by amalgamation and then inserting the tip for about 8 hours into dry mercury.

The electrode preparation was terminated by a slight alignment of the mouth followed by brushing or cleaning. For the gradual purification, water from the natural water tank after decantation (VD) containing about 0,1 $mg \cdot L^{-1}$ C10-C40, 41 $mg \cdot L^{-1}$ Ca, 14 $mg \cdot L^{-1}$ Mg, 5 $\mu g \cdot L^{-1}$ Cu, 1 $\mu g \cdot L^{-1}$ Cd, 39 $mg \cdot L^{-1}$ Cl, 7 $mg \cdot L^{-1}$ NO_3, 57 $mg \cdot L^{-1}$ SO_4^{2-}, 12 $mg \cdot L^{-1}$

SiO_2, 75 μg·L^{-1} AOX, pH ~7,5 was used. The (VD) was conditioned by coagulation and filtration (VKF) after the cation exchange column (VK) and the anion exchange column (VA), then collected and stored in the water reservoir (VZ). Lewatit S 100 (Lanxess, Cologne, Germany) served as a cation, with a mean particle size of about 640 μm. The annex column contained a slightly basic Lewatit MonoPlus MP 64 (Lanxess, Cologne, Germany) with a mean particle size of about 600 μm, mixed in a 1:1 ratio with a strongly basic anion of Lewatit MonoPlus M 600 (Lanxess, Cologne, Germany) with a mean particle size of about 610 μm. Stock solutions of 0.1 M and 1 M $AgNO_3$ (Merck, Germany) and other solutions were prepared using demineralized water with a conductivity of < 0.1 μS·cm^{-1}. Prior to the measurement, the solution was bubbled with a nitrogen purge for 5 minutes and the nitrogen was fed over the solution during the measurement. The measurements were carried out at 293 K.

2.1.2 Measurements using the zinc amalgam electrode for the detection of concentration changes of zinc sulphate by nanofiltration

The potentiometric experimental arrangement included a cell and a stand of the Eco-Tribo Polarograph (Eco-Trend Plus, Prague) and accessories, an industrial digital multimeter IP67 (EXTECH Instruments, USA) connected via a special input/output interface[17,18] to the Zinc and Zinc Amalgam Electrodes (ZnE or ZnAE) and the reference mercury sulphate electrode. All the three electrodes, an electromagnetic stir bar, and a gas-inlet were inserted into the solution in a closed glass cell. The solutions were prepared from demineralized water (< 0.1 μS·cm^{-1}, from the Milli-Q Plus water-purification system, Millipore, Bedford, USA) and reagent-grade chemicals. The linear least-square regression in Origin Pro 7.5 (OriginLab Corporation, USA) was used for fitting calibration curves and the relevant results (slope and intercept) were reported with a confidence interval of 95 % probability.

The nanofiltration experiments were carried out using small aqueous samples from 25 to 170 mg·L^{-1} Zinc Sulphate ($ZnSO_4$) and a tubular nanofiltration arrangement of a cross-flow separation unit which has been described in detail elsewhere[5,6,31]. A commercially available type of membrane made of poly-amid film, AFC 40, PCI

Membrane Systems (Poland), was used. Effective membrane area was 240 cm^2 (two tubes, each with a length of 30 cm and an internal diameter of 1.25 cm, pH ranged from 1.5 to 9.5 and maximum temperature of 333 K).

2.2 Experimental conditions under which the treated data on agglomeration processes were collected

2.2.1 Assessment of the agglomeration kinetics of waste nanoparticles based on its partial similarities with the electrosorption processes

The adsorption data of sodium thiosulfate at the constant potential E = -0.1 V versus SCE (Sodium Chloride Electrode) in a concentration range of its surface access Γ between $0.4 \cdot 10^{-6}$ and $2 \cdot 10^{-6}$ $mol \cdot m^{-2}$ were obtained by the improved controlled convection drip-time technique CCDT[10,32] using a glass spindle capillary with drop time of about 70 s. The solution was stirred during the drop-growth to ensure the attainment of adsorption equilibrium; as a result, the stirrer was stopped at about 10 s before the fall of the drop. The reproducibility of the CCDT method was better than ± 0.3 $mN \cdot m^{-1}$.

The electrocapillarity measurements were calibrated assuming that the electrocapillary maximum in the base electrolyte was γ = 426.7 $mN \cdot m^{-1}$ at 293.2 K. Repeatability of Γ versus c concentration of sodium thiosulfate was better than ± 10 %. The experimental arrangement included PC-controlled voltammetric analyzer PC-ETP (Eco-Trend Plus Co., Czech Republic[26-28,33]), a laboratory-made electrocapillary arrangement and a digital counter for the drop-time measurements. The stock solution was 1 mM of nAg, prepared by a modified Tollens process[34] based on the chemical reduction of silver nitrate ($AgNO_3$) by glucose ($C_6H_{12}O_6$). The studied solution of nAg[34] of a concentration 10 $\mu mol \cdot L^{-1}$ was prepared using dilution of the stock solution by liquid Medium 203 and its concentration was verified by the optical emission spectroscopy (OES) with inductively coupled plasma (ICP-OES). The medium 203 was the aqueous solution containing 2 mM $CaCl_2$, 0.5 mM $MgSO_4$, 0.77 mM $NaHCO_3$ and 0.075 mM KCl. Its pH value was 6.8. The hydrodynamic diameters (D_H) were measured[34] by dynamic light scattering (DLS) with ZetaPALS Potential Analyzer

(Brookhaven Instruments Corp., USA). The experimental set-up of the OES with ICP-OES[34] was done using the instrument IntegraXL2 (GBC, Dandenong, Australia). The pH was measured by the portable laboratory arrangement. The solutions used were prepared from bidistilled water and reagent grade chemicals (Sigma-Aldrich). Thiosulfate anions were added in the form of their sodium salt $Na_2S_2O_3$. The aqueous solutions were stored at laboratory temperature. The working standard solutions were prepared daily by dilution of the stock solutions.

2.3 Statistical data analysis of experimental data

The experimental data were analyzed and graphically represented using the Statistica software (version 13), OriginPro software (version 7.5) and Microsoft Excel 2010 respectively.

3. RESULTS AND DISCUSSION

3.1 Utilization of changes in the Nerstian potentiometric behaviour of silver amalgam electrodes AgAE during ion exchange water treatment

3.1.1 Background of the study

The most significant advantages of potentiometry in the field of water and waste management, for example, when monitoring the pH or metal content, are its relative simplicity, availability and operational applicability[2,3,8]. The new knowledge of its use is therefore of great interest, especially if it can be applied sooner or later under normal (operational) conditions. Water purification methods and control procedures are many. As to the common technological conditions, conductometry is the most preferable technique used for pure water quality control[1-3,7,8]. Generally, in principle, when monitoring the water treatment process, the control system, in particular, develops a flow chart in a sequence of individual cleaning steps when passing the sample from one purification step to the sample from the following step. If the character of such a diagram is sufficiently pronounced and repeatable, then the control system requires further research attention. Therefore, the water purification processes used, in particular, may be associated with relatively pure water accompanied by the release of relatively trace amounts of substances for which a single control method – otherwise

widely used – is less sensitive. Then, the use of two control methods (systems) operating on mutually independent principles is recommended in such cases. Such a situation may occur, for example, water purification using organic ion exchangers. Column traces, which can be released particularly through a more demanding long-lasting cleaning regime, can be low-polar substances with low or inadequate detection conductivity sensitivity. For this purpose, it was recently proposed[14,15,19] to test the behaviour of modified new types of solid amalgam electrodes that have been introduced successfully in voltammetry[10-13,29,35-37] and also rarely tested in potentiometry[14,19].

3.1.2 Results and discussion

All potentiometric measurements were performed by adding 1 ml of 0.1 M $AgNO_3$ stock solution to 10 ml of the collected water sample so that the $AgNO_3$ content of the sample was 0.007 $mol \cdot l^{-1}$. Samples were sequenced, starting with decantated water (VD), water after coagulation and filtering (VKF), water after cation (VK), using anion (VA) and water from the reservoir (VZ). As the samples varied considerably from each other, the anions, cations and organic substances contained in them varied to the Ag^+ ions hence reduced the activity of these ions. In the case of the AgAE, both Hg_2^{2+} and Hg^{2+} ions were active concurrently to Ag^+. Hg^{2+} was present near the surface of the electrode. Therefore, in the transition from one sample to another, greater changes in the mixed potentials *E* in the case of AgAE were observed. As a result of this, the sensitivity and repeatability of AgAE were better than that of AgE. The results[14] are documented in the following figures. Figure 1 shows the three repeated measurements of potential *E* of samples in the order V1, V2, V3, V4 and V5 for the corresponding VD, VKF, VK, VA and VZ using AgE. The diagrams of potential *E* versus *Vi* showed poorly repeatable waveforms that did not have characteristic courses in the sequence from V1 to V5.

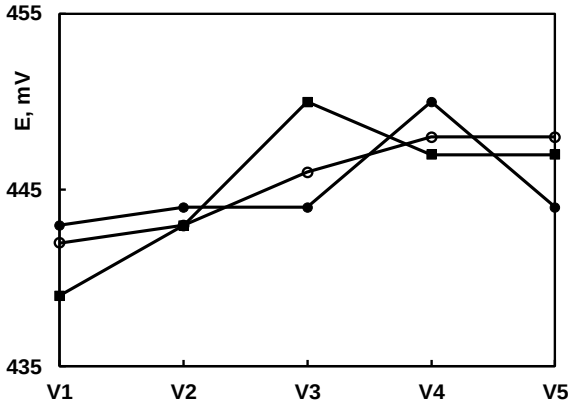

Figure 1 - *E* versus *Vi* diagrams of three repeated measurements on the silver electrode (AgE)

However, for AgAE as shown in Figure 2, the course of the potential *E* versus *Vi* was significantly different. The diagrams obtained had satisfactory repeatability and the character of their course was quite reproducible.

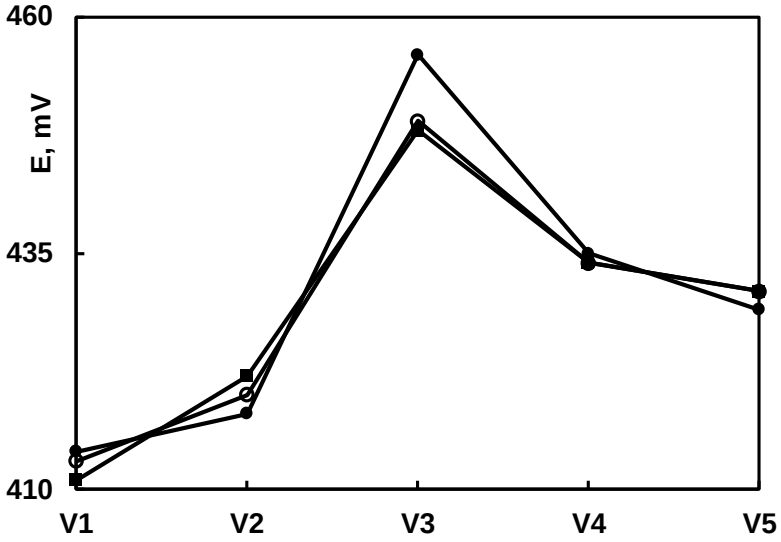

Figure 2 - *E* versus *Vi* diagrams of three repeated measurements on the silver amalgam electrode AgAE

One reason for the AgE behaviour can be attributed to the fact that Ag^+ ions exhibit significant interactional activity in the solution not only against many anions but also with organic components. Surface layers of chemical products of cations and anions could even act as a filter against most of the interfering organic components present in V1 and V2, however, their influence often causes other components into the monitored solutions to which the SE may also be sensitive. The oxidative attack of the strongly

acidic cation system according to the scheme in Figure 3, for example, is accompanied by hydrolysis and molecular segments of exchanges are released[38].

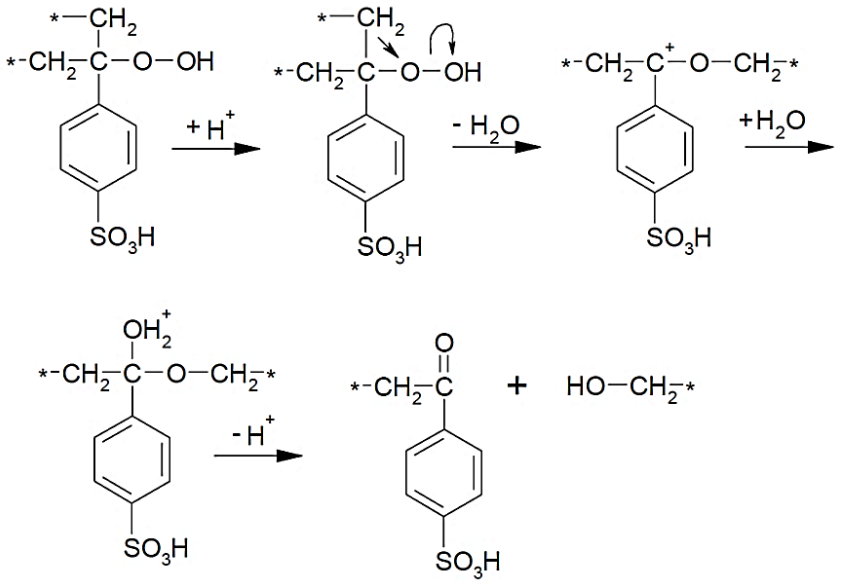

Figure 3 - Oxidation attack of the strongly acidic cation exchanger

Other events that are applied to the anion are dealkylation of its functional groups[39] by the temperature according to the scheme in Figure 4.

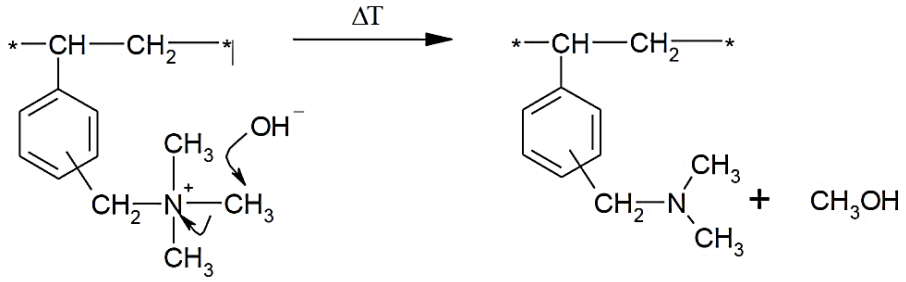

Figure 4 - Dealkylation of the anion exchangers

Similarly, traces of organics may be released in the presence of humic acids in their interactions[40] with the strongly basic anion according to the scheme in Figure 5.

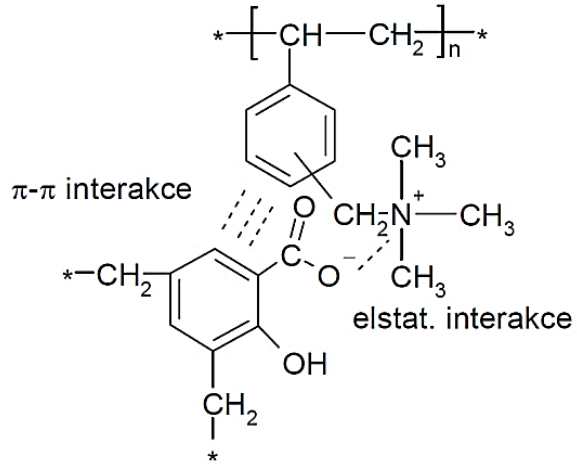

Figure 5 - Interaction of humic acid with a strongly basic anion exchanger

These interactions with organic solvents can also be applied to AgAE. However, as the results of the measurements showed, the extent of the manifestations of the disturbing events by this electrode was considerably limited compared to AgE. In addition to the differences in material composition, great differences in surface quality could have contributed to this, which is significantly smoother (compared to polished AgE) and is more isotropic than AgE surface. Schematically, the potential changes *E* (cited in[14]) by AgE are based on Eqs. 1 and 2 as follows:

$$E_{Ag} = E^0_{Ag} + \frac{RT}{F} ln a_{Ag^+} \quad \text{Eq. 1}$$

$$E_{Ag/AgY} = E^0_{Ag/AgY} - \frac{RT}{F} ln a_{Y^-} \quad \text{Eq. 2}$$

where *Y* denotes the solution component integrating with Ag^+; *R*, *T* and *F* are universal gas constant, absolute temperature and Faraday constant. Similarly, Eqs. 3, 4 and 5 can be written based on the mixed potential *E* of the AgAE electrode.

$$E_{Ag(Hg)} = E^0_{Ag(Hg)} + \frac{RT}{F} ln a_{Ag^+} \quad \text{Eq. 3}$$

$$E_{Hg} = E^0_{Hg} + \frac{RT}{2F} ln a_{Hg_2^{2+}}, \quad \text{Eq. 4}$$

$$E_{Hg/Hg_2Y_2} = E^0_{Hg/Hg_2Y_2} - \frac{RT}{F} ln a_{Y^-} \quad \text{Eq. 5}$$

Furthermore, the surface of AgAE did not require renewal or restoration earlier than after the first and second week, unlike the AgE, which was mechanically or practically restored before each series of measurements. However, for the renewal of the AgAE surface, usually, it was enough to wipe the face of the electrode slightly. The results

have shown that continuing research in the direction discussed earlier may need further improvements.

3.2 Utilization of the potentiometric signal of the zinc amalgam electrode ZnAE for the detection of concentration changes of dissolved $ZnSO_4$ by nanofiltration

3.2.1 Background of the study

The study of nanofiltration of aqueous solutions has made much progress during the past 20 years[31]. One of the most attractive results is its success in possible separation of ionic heavy metals or other molecular pollutants, which can be applied, for example, in the treatment of drinking, waste or industrial waters and effluents[5,6,31,41]. One of the well-known metallic pollutants[42] is zinc present in the form of its divalent ions. Zn is an essential element necessary for living organisms. It is important, for example, for a proper functioning of the immune system, enzymes and DNA synthesis or gene expression. On the other hand, its uptake by human above a certain level causes some acute and chronic illness, fever, gastroenteritis, anaemia, renal failure, allergies, and internal organ damage[43]. The limit for zinc in waste-water according to the National Secondary drinking Water regulation of the EPA[44] is 2.61 $mg \cdot L^{-1}$, which is in good agreement with that of 1.5 to 3 $mg \cdot L^{-1}$ valid in the Czech Republic[45]. Zinc concentration is rising in the environment. It is released by electrotechnical industry, electroplating, mining, metallurgical, and pharmaceutical and paint production, coal-power stations as well as from other industrial production and use, for example, catalysts.

Recent studies[5] have outlined some relevant technological applicability of nanofiltration using a pressure-driven membrane[6,46,47] for separation of zinc[48-50] (or its salts) provided that the proper arrangements and working parameters (like the type of the thin-film composite membrane, cross-flow velocity, pressure, temperature, flow-rate, etc.) can be verified experimentally. It simply means that many experiments must be accompanied by several analyses focused on the determination of the input/output ratio of the analyte concentrations.

For these purposes (regardless of the required independent analytical background); the rapid, relatively simple, disposable and low-cost techniques and applicability (proximity); are desirable for reducing the corresponding effort, time and cost associated with its application. Recently[14,19,51], such methods and arrangements for the purposes described were suggested based on potentiometry with a modified new generation of the detection metal amalgam electrodes or sensors. For zinc, in well-equipped analytical laboratories, the available methods for its determination include inductive coupled plasma-optical emission spectroscopy (ICP-OES), atomic absorption spectrometry (AAS), ICP-mass spectrometry (ICP-MS)[52,53], potentiometry, and voltammetry[3]. As indicated, potentiometry could principally meet the above-mentioned demands on the condition that the proper detection electrode is found. However, at present, zinc ion selective electrode is not commercially available. On the other hand, the last two decades have shown much progress in the application of voltammetry by using a new generation of solid (or modified) amalgam electrodes[11-13,35,36]. And some recent communications or notes[14,19,51] concerning the advanced special (or modified) amalgam electrodes (AE) (including AgAE, CuAE, ZnAE etc.) have outlined their new possibilities in the field of potentiometry, as well. Nevertheless, as for ZnAE, there is basic or relevant experimental data regarding its application in this respect. Thus, the work aimed at presenting basic testing of a potentiometric sensitivity of the zinc solid amalgam electrode (ZnAE) (partly in comparison with a zinc electrode, ZnE) with respect to concentration changes of $ZnSO_4$ in aqueous solutions, among others under the experimental conditions similar to those applied by using the nanofiltration technologies.

3.2.2 Results and discussion

In comparison with ZnE, the system with ZnAE reached the quasi-steady state more rapidly and its stability was much better. However, as expected, certain irreproducibility of *E-t* dependences were observed, as well. The consecutive *E-t* plots as shown in Figure 6 at different concentrations of $ZnSO_4$ from $1 \cdot 10^{-4}$ to $1 \cdot 10^{-1}$ $mol \cdot L^{-1}$ confirmed the above-mentioned advantages of ZnAE compared to ZnE. It implies that after the ZnAE was inserted into the solutions, the measured potentials *E* reached their

quasi-constant values in 250 to 300 s, which can be utilized analytically. Therefore, further measurements of *E* with ZnAE in solutions containing various concentrations of $ZnSO_4$ were performed in 300 s after the electrode was inserted into the solution. In this way, the calibration *E-log c* dependence (see Figure 7) in a concentration range from $5 \cdot 10^{-5}$ to $1 \cdot 10^{-2}$ mol·L^{-1} of $ZnSO_4$ was obtained. A linear relationship between potential *E* and *log c* exhibited an analytically utilizable slope $\delta E / \delta \log c$ = -35.9 mV. The reason for the decrease of the *E* versus *log c* dependence is probably connected with a complex of present interactions and reactions including the formation of insoluble salts, hydroxides, oxides, or other products on the electrode. The obtained *E-log c* dependences shifted a little of the potential while maintaining their slope and the linear relationship between potential and the logarithm of concentration. The finding was confirmed by further analysis of the data as summarized in Table 1.

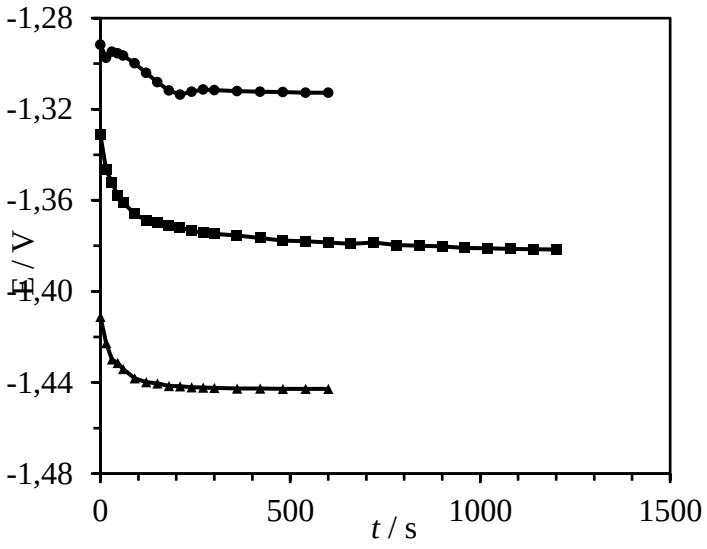

Figure 6 - The *E-t* plot on ZnAE corresponding to concentrations $1 \cdot 10^{-4}$ mol·L^{-1}(•), $1 \cdot 10^{-3}$ mol L^{-1}(■); $1 \cdot 10^{-1}$mol·L^{-1}(▲) $ZnSO_4$

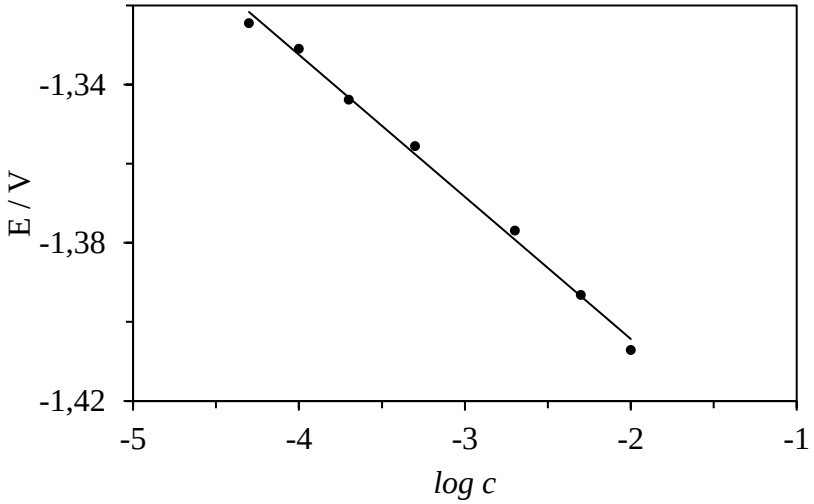

Figure 7 - Calibration of *E-log c* dependence in $ZnSO_4$ using ZnAE

$$E = -(0.0359 \pm 0.0011) \cdot log\ c - (1.4761 \pm 0.0037)$$

Table 1 - Repeated potentiometric calibration measurements of ZnAE in $ZnSO_4$

c (mol·L^{-1})	*log c*	E (V)
$1 \cdot 10^{-4}$	-4.0000	-1.3436
$2 \cdot 10^{-4}$	-3.6990	-1.3491
$5 \cdot 10^{-4}$	-3.3010	-1.3570
$1 \cdot 10^{-3}$	-3.0000	-1.3757
$2 \cdot 10^{-3}$	-2.6990	-1.3750
$5 \cdot 10^{-3}$	-2.3010	-1.3927
$1 \cdot 10^{-2}$	-2.0000	-1.4053
$2 \cdot 10^{-2}$	-1.6990	-1.4195
$5 \cdot 10^{-2}$	-1.3010	-1.4385

$$E = -(0.0351 \pm 0.0021) \cdot log\ c - (1.4775 \pm 0.0037)$$

Further potentiometric measurements utilizing the above-mentioned constant slope value of the *E-log c* calibration curve were employed to estimate the efficiency in nanofiltration applied on five model samples containing input zinc concentrations c_i (mg·L^{-1}): 26; 51; 101; 151 and 167 respectively. According to ICP-OES, the

corresponding output concentrations c_{out} (mg·L^{-1}) were 0.7; 0.7; 1.3; 1.8 and 1.6 respectively. On the basis of the known input concentration *ci*, the slope of *E-log c* and the measured potential differences ΔE_i corresponding to every couple of "input-output" of all the samples potentiometrically estimated, the corresponding output concentrations c_{out} were < 2 mg·L^{-1}. For all the measurements, calibration or other analyses with the ZnAE were performed without any treatment, maintenance or renewal of its surface during the measurements.

3.3 Characterization of the kinetics of silver particles agglomeration

3.3.1 Background of the study

In recent years, silver nanoparticles or sub-microparticles (or colloidal agglomerates) have gained significant applications in the textile and food industry, pharmaceutical products and household appliances[54]. The colloidal nanosilver solution based on a silver nanomaterial has the potential for practical applications in the anti-bacterial treatment. However, its potential toxicity, content in water and the ratio between the content of silver in colloidal agglomerates in its soluble ionic form Ag^+ has raised an immediate attention of researchers. In fact, thanks to the antibacterial effects, colloidal solutions of nanosilver[55] as disinfectants have been used for centuries to combat infectious diseases, such as traumatic, diabetic or chronic infected wounds[56]. The Woodrow Wilson database contained 259 commercially available products with silver nanoparticles in 2010. The increase in their production[57] resulted in an increased risk of silver toxicity on the environment and potential impacts on human health. Generally, electrochemical composites made of silver powder have proven to be good electrode material[11,12,69-73], usable like mercury[58-61] for the study or analysis of a series of bioactive species.

In the literature, the study of silver nanoparticles or sub-microparticles toxicity has received little attention[62] and results of terrestrial studies as well as laboratory tests of ecotoxicity are unclear[34,63], because the toxicity of silver colloidal agglomerates is obviously influenced by a wide range of factors, such as particle size, ionic composition of the solution, pH, presence of other components of the solution, etc.

For instance, the reaction of minor aquatic organisms for the presence of Ag indicates a considerable influence of particle size on the harmful effects of silver colloidal agglomerates. Considering the various factors mentioned above, the size of silver nanoparticles or sub-microparticles and the evaluation of kinetics of the particles growth depending especially on silver concentration and time are of primary importance. Fitting the time-dependence of the silver nanoparticles or sub-microparticles diameter D was carried out in the range of 0 to 250 minutes. The aim of the study was to investigate the concentration and time dependent changes of diameter D using the spectroscopic analysis combined with the atomic force microscopy and dynamic light scattering[23,34]. As shown in Figure 16[22,23,34], significant changes in D occurred within the time span of more than 200 minutes approaching their limit values D_{inf} of hundreds of nanometres (nm). As a result of the rapid formation of the primary nucleus at a time t_0 (close to 0 seconds) dependencies in Figure 8 at the beginning did not pass through the point at $D = 0$. The most significant changes to the size D on time subsequently occurred in the range between 0 and 100 minutes.

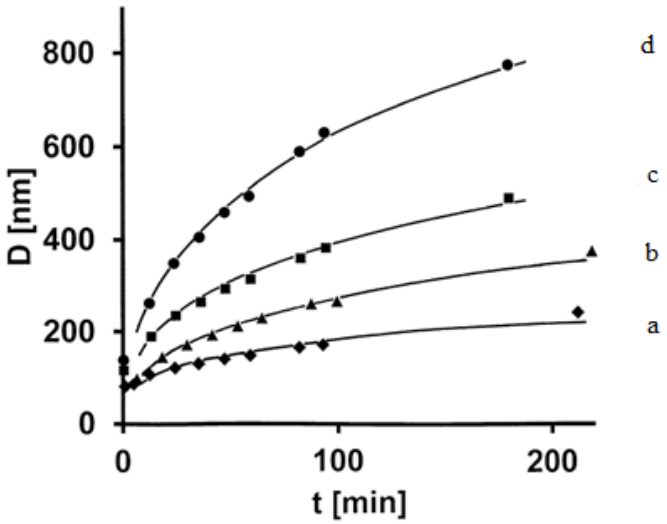

Figure 8 - Kinetics of the growth of silver nanoparticles (diameter D versus time t) for concentrations of (a) 5 μM (b) 10 μM (c) 25 μM (d) 50 μM

3.3.2 Results and discussion

In this respect, the behaviour of the systems resembled that of the adsorption type of a quantity of surface active species[10] which (under appropriate conditions) provided adsorption isotherms (i.e. dependencies of surface concentration of the substance Γ on its volume concentration c) not starting from the beginning of coordinates. In view of this, the analysis of kinetic growth and fitting of the appropriate curves were performed, separately for silver concentrations 25 μM and 50 μM. This was based on the assumption that the changes in D with time often correspond approximately to the model (Eq. 6)[34].

$$ln[(D_{inf} - D)/(D_{inf} - D_0)] = -k\,t \qquad \text{Eq. 6}$$

The measured data for 25 μM Ag, the magnitude $y = ln[(D_{inf} - D)/(D_{inf} - D_0)]$ versus t for gradually selected values of D_0 at ($t_0 \to 0$) from 20 nm to 100 nm and $D_{inf} = 510$ nm (estimated from Figure 8) were linearized (Table 2). The optimum linearization $y = kt + q$, at correlation coefficient R, using OriginPro 7.5 (OriginLab Corporation, USA) was reached at $D_0 = 50$ nm and $D_{inf} = 510$ nm, respectively.

Table 2 - Linearization parameters k, q, R of $y = kt + q$ following Eq. 6; 25 μM Ag; $D_{inf} = 510$ nm; q – intercept

D_0 (nm)	k (min^{-1})	q	R
20	–0.0159±0.0010	–0.0765±0.0754	0.9824
30	–0.0159±0.0010	–0.0601±0.0749	0.9825
40	–0.0159±0.0010	–0.0434±0.0745	0.9826
50	–0.0158±0.0010	–0.0264±0.0742	0.9828
60	–0.0158±0.0010	–0.0090±0.0741	0.9826
70	–0.0157±0.0010	–0.0089±0.0741	0.9825
80	–0.0157±0.0010	–0.0271±0.0742	0.9823
90	–0.0156±0.0010	–0.0457±0.0745	0.9821
100	–0.0156±0.0010	–0.0648±0.0750	0.9818

The extrapolated value of the diameter D_0 corresponded to the above mentioned diameter of the initial nucleus D_0 obtained using atomic force microscopy. Following Eq. 6 for $D_0 = 50$ nm the value of k was -0.0158 ± 0.0010 [min^{-1}] and the intercept q was -0.0264 ± 0.074. The evaluated uncertainty in values of the mentioned coefficients were apparently associated with the application of other factors (inter-particle interactions, the combination of the type of transport processes, etc.) which influenced the kinetics of the particles growth. Hence, the obtained slopes for k using Eq. 6 represented in fact their average values. For different nature of the nucleation processes close to $t \to 0$ and in opposite to the steady state processes at higher t, the linearization of experimental data was carried out starting from the first experimental value D_1 at t_1 (see the first experimental point in Figure 8). The aim was to obtain parameters k_1, q, R under the steady growth of silver nanoparticles. The model Eq. 7 was utilized.

$$ln[(\Delta D_{inf} - \Delta D_i)/(\Delta D_{inf} - \Delta D_1)] = k_1(t_i - t_1) = k_1 \Delta t_i \qquad \text{Eq. 7}$$

where $\Delta D_i = D_i - D_1$, $\Delta t_i = t_i - t_1$, $\Delta D_{inf} = D_{inf} - D_1$. From the experimental data, the values $\Delta y_i = ln[(\Delta D_{inf} - \Delta D_i)/(\Delta D_{inf} - \Delta D_1)]$ vs. $\Delta t_i = t_i - t_1$ were consecutively plotted. Dependencies Δy_i vs. Δt_i were then linearized at different estimated values ΔD_{inf} in the range of 450 nm to 600 nm. The resulting linearization parameters are summarized in Table 3. They indicated that the optimum linearization was achieved at $\Delta D_{inf} = 480$ nm.

Table 3 - Linearization parameters k_1, q, R of Δy_i vs. Δt_i following Eq. 7 and Figure 16; 25 μM Ag

ΔD_{inf} (nm)	k_1 (min^{-1})	q	R
450	–0.0096±0.0002	–0.0361±0.0173	0.9958
480	–0.0081±0.0002	–0.0571±0.0145	0.9959
500	–0.0074±0.0002	–0.0649±0.0155	0.9943
550	–0.0061±0.0002	–0.0739±0.0181	0.9887
600	–0.0052±0.0002	–0.0760±0.0193	0.9826

At this optimal value ΔD_{inf} a segmented linearization of Δy_i vs. Δt_i was then applied[24]. It consisted of gradual linearization of segments of Δy_i vs. Δt_i (see Eq. 7 and the points in Figure 8), or more exactly of the following consecutive sets of always five successive points: 1st set [$(0; 0)$; $(\Delta t_1; \Delta y_1)$; $(\Delta t_2; \Delta y_2)$; $(\Delta t_3; \Delta y_3)$; $(\Delta t_4; \Delta y_4)$]; 2nd set [$(\Delta t_1; \Delta y_1)$; $(\Delta t_2; \Delta y_2)$; $(\Delta t_3; \Delta y_3)$; $(\Delta t_4; \Delta y_4)$; $(\Delta t_5; \Delta y_5)$]; 3rd set [$(\Delta t_2; \Delta y_2)$; $(\Delta t_3; \Delta y_3)$; $(\Delta t_4; \Delta y_4)$; $(\Delta t_5; \Delta y_5)$; $(\Delta t_6; \Delta y_6)$]; 4th set [$(\Delta t_3; \Delta y_3)$; $(\Delta t_4; \Delta y_4)$; $(\Delta t_5; \Delta y_5)$; $(\Delta t_6; \Delta y_6)$; $(\Delta t_7; \Delta y_7)$]; 5th set [$(\Delta t_4; \Delta y_4)$; $(\Delta t_5; \Delta y_5)$; $(\Delta t_6; \Delta y_6)$; $(\Delta t_7; \Delta y_7)$; $(\Delta t_8; \Delta y_8)$]. The results of the segmented linearization are shown in Table 4.

Table 4 - Segmented linearization of five sets of $\Delta y_i \; vs. \; \Delta t_i$ data (see points in Figure 8 and Eq. 7), i.e., following consecutive sets of five successive points $(\Delta t_i; y_i)$: 1st set, $i = 1, 2, 3, 4, 5$; 2nd set, $i = 2, 3, 4, 5, 6$; 3rd set, $i = 3, 4, 5, 6, 7$; 4th set, $i = 4, 5, 6, 7, 8$; 5th set, $i = 5, 6, 7, 8, 9$; $\Delta D_{inf} = 480$ nm

Number of sets	$k_1(\text{min}^{-1})$	q	R
1.	–0.0092±0.0007	–0.0258±0.0203	0.9886
2.	–0.0075±0.0004	–0.0799±0.0158	0.9942
3.	–0.0068±0.0001	–0.1101±0.0063	0.9994
4.	–0.0070±0.0001	–0.1049±0.0098	0.9991
5.	–0.0072±0.0001	–0.0899±0.0088	0.9997

This implies that the time constants by (variable Δt) for individual segments were not quite constant in fact since they were more or less changing during the progress of agglomeration (and therefore also with t). It can be assumed that one of the reasons of the variations of k_1 (see Eq. 7) in the case of the different mentioned segments of the given dependence is the fact that the behaviour of the system does not meet exactly the conditions valid for kinetic equations of the first order. The latter equations are rather useful for approximation in the given case. This explanation is consistent with that of the adsorption/agglomeration processes[10,24] at interfaces where strong mutual interactions of particles, reorientation, etc., occurred. For these reasons, the equations

(Eq.8) and (Eq.9), originally suggested[10,24] for evaluation of adsorption data could alternatively be applied for fitting or describing of agglomeration processes, as well.

$f_1(Y)\ exp\ f(Y) = k\ X$ Eq. 8

$-ln(1-Y) = K(t)c$ Eq. 9

where variable $Y = D/D_{inf}$, $X = t$ or $(t-t_1)$, $K = K(t)$, $c = c_0 = \text{constant}$ or $c = c(t)$. Although both concentrations (25 μM Ag and 50 μM Ag) showed similar types of dependences, their parameters were different. Their linearization $\ln[(D_{inf}-D)/(D_{inf}-D_0)]$ versus t according to Eq. 6 for selected values of D_0 varying between 20 nm and 100 nm resulted to the estimation of the optimum D_0 between 30 and 50 nm (Table 5).

Table 5 - Linearization parameters k, q, R of $y = kt + q$ following Eq. 6; 50 μM Ag; $D_{inf} = 800$ nm; q – intercept

D_0 (nm)	k (min^{-1})	q	R
20	–0.0176±0.0008	–0.0383±0.0617	0.9901
30	–0.0176±0.0008	–0.0280±0.0615	0.9902
40	–0.0176±0.0008	–0.0176±0.0614	0.9902
50	–0.0175±0.0008	–0.0071±0.0613	0.9902
60	–0.0175±0.0008	–0.0036±0.0613	0.9901
70	–0.0175±0.0008	–0.0144±0.0614	0.9901
80	–0.0175±0.0008	–0.0254±0.0615	0.9900
90	–0.0174±0.0008	–0.0365±0.0617	0.9899
100	–0.0174±0.0008	–0.0478±0.0620	0.9910

For $D_0 = 50$ nm and $D_{inf} = 800$ nm (estimated from Figure 8), the analogous linearization produced the average time constant $k = -0.0175 \pm 0.0008\ [\text{min}^{-1}]$. By plotting the analogous dependencies of $y_i = ln[(\Delta D_{inf}-\Delta D_i)/(\Delta D_{inf}-\Delta D_1)]$ versus $\Delta t_i = t_i - t_1$ for 50 μM Ag and their linearization according to Eq. 7 for selected values D_{inf} between 700 and 900 nm produced the data summarized in

Table 6. The maximum value of the correlation coefficient R corresponded to the value $\Delta D_{inf} = 700$ nm.

Table 6 - Linearization parameters k_1, q, R of $\Delta y_i \; vs. \; \Delta t_i$ following Eq. 7 and Figure 16; 50 μM Ag

ΔD_{inf} (nm)	k_1(min^{-1})	q	R
700	–0.0131±0.0002	–0.0079±0.0189	0.9986
750	–0.0104±0.0002	–0.0608±0.0177	0.9981
800	–0.0087±0.0003	–0.0823±0.0251	0.9946
850	–0.0076±0.0004	–0.0919±0.0287	0.9907
900	–0.0067±0.0004	–0.0959±0.0302	0.9870

The results of the segmented linearization (similar to Table 6) of Δy_i vs. Δt_i for 50 μM Ag and for $\Delta D_{inf} = 700$ nm are shown in Table 7. In this case the time constant k_1 by variable Δt (in Eq. 7) was to some extent time-dependent, as well.

Table 7 - Segmented linearization of five sets of $\Delta y_i \; vs. \; \Delta t_i$ data (see points in Figure 8 and Eq. 7), i.e., following consecutive sets of five successive points $(\Delta t_i; y_i)$: 1st set, $i = 1, 2, 3, 4, 5$; 2nd set, $i = 2, 3, 4, 5, 6$; 3rd set, $i = 3, 4, 5, 6, 7$; 4th set, $i = 4, 5, 6, 7, 8$; 5th set, $i = 5, 6, 7, 8, 9$; $\Delta D_{inf} = 700$ nm

Number of sets	k_1 (min^{-1})	q	R
1.	–0.0130±0.0007	–0.0252±0.0203	0.9941
2.	–0.0112±0.0006	–0.0817±0.0220	0.9948
3.	–0.0115±0.0005	–0.0782±0.0284	0.9956
4.	–0.0126±0.0006	–0.0209±0.0422	0.9949
5.	–0.0136±0.0003	–0.0563±0.0270	0.9992

Following Eq. 6 the fitting kinetics of silver nanoparticles agglomeration with time was further evaluated using forward stepwise regression analysis[64,65]. The results are shown in Tables 8 to 11 and Figures 9 to 12 respectively.

Table 8 - Regression summary of the dependent variable *y*

N=180	b*	Standard Error of b*	b	Standard Error of b	t-value	p-value $\alpha = 0.05$
Intercept	-	-	0.013691	0.043637	0.3138	0.754076
t (min)	- 0.984674	0.012267	- 0.016629	0.000207	- 80.2686	0.000000
D_0 (nm)	0.047443	0.012267	0.001610	0.000416	3.8675	0.000155
c_D_{inf} (μM)	- 0.041004	0.012267	- 0.002875	0.000860	-3.3426	0.001014

N=Number of samples; t = time; D_0 = diameters; c_D_{inf} = concentration at maximum diameters; b* = standardized regression coefficients; b = raw regression coefficeints; t-value = measures the size difference relative to the variation in data; p-value = significance level used for testing a statistical hypothesis; α = significance level

Table 9 - Summary statistics of the dependent variable *y*

Statistic	Value
Multiple R	0.986668451
Multiple R^2	0.973514633
Adjusted R^2	0.973063177
F	2156.39291
p	0.000000
Standard Error	0.144252687

R = Correlation coefficient, R^2 = Coefficient of determination**,** F-value = value of the F test used in combination with the p-value to measure significance

Table 10 - Regression summary of the dependent variable D_H

N=180	b*	Standard Error of b*	b	Standard Error of b	t-value	p-value $\alpha = 0.05$
Intercept	-	-	-35.3427	19.15861	-1.84475	0.066746
t (min)	0.824815	0.030784	2.9726	0.11094	26.79324	0.000000
c_D_{inf} (μM)	0.389794	0.030784	5.8325	0.46063	12.66205	0.000000

D_H = hydrodynamic diameter (nm)

Table 11 - Summary statistics of the dependent variable D_H

Statistic	Value
Multiple R	0.912282909
Multiple R^2	0.832260106
Adjusted R^2	0.83036474
F	439.102575
p	0.000000
Standard Error	77.2499755

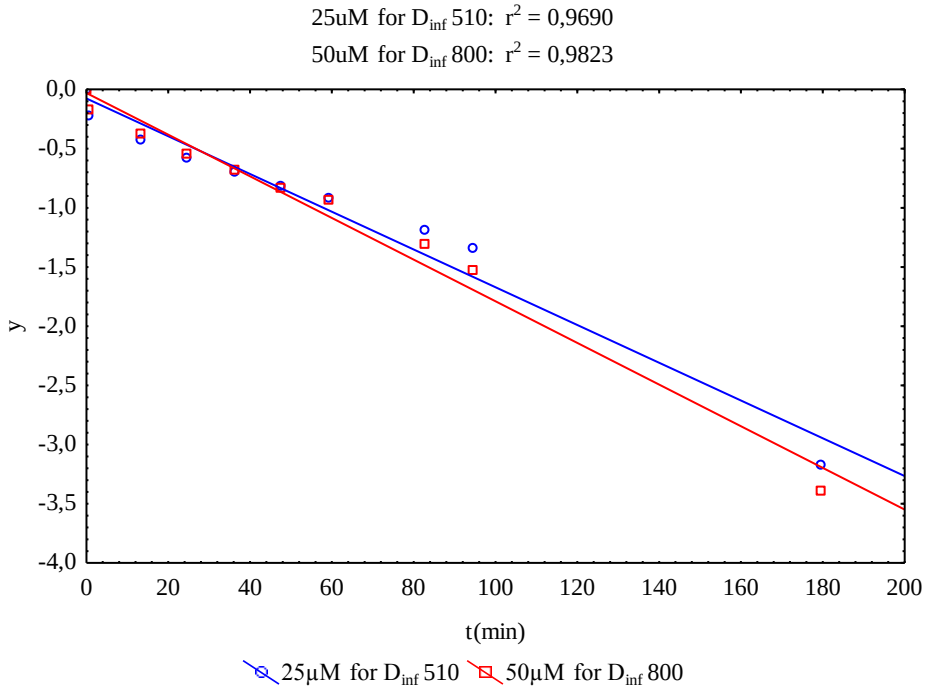

Figure 9 - 2D scatterplots of *y* versus *t* at D_0 20 (nm) in relation to different concentrations *c* of 25 µm of D_{inf} 510 and 50 µm of D_{inf} 800

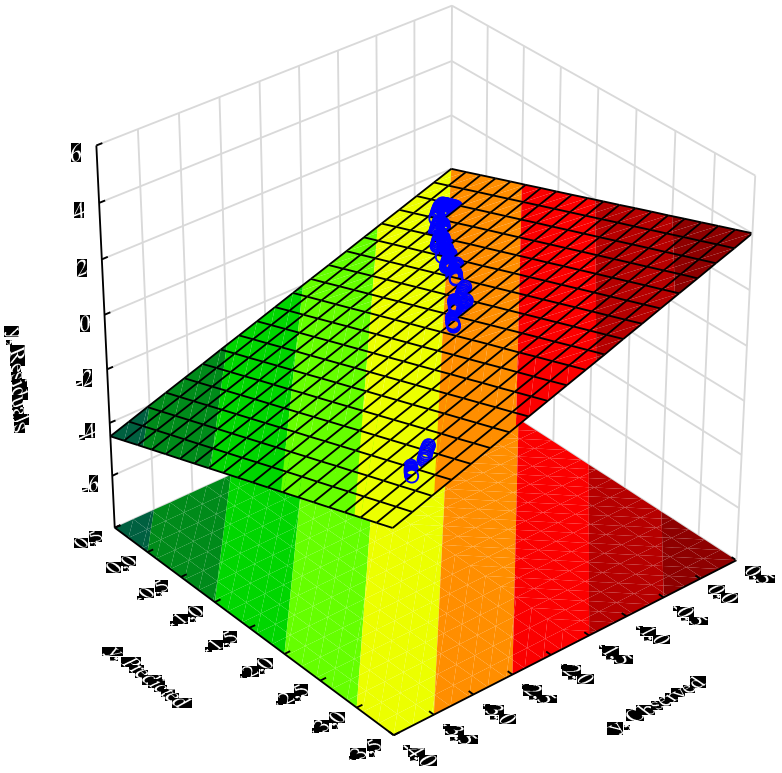

Figure 10 – Dependent variable y observed versus predicted versus residuals

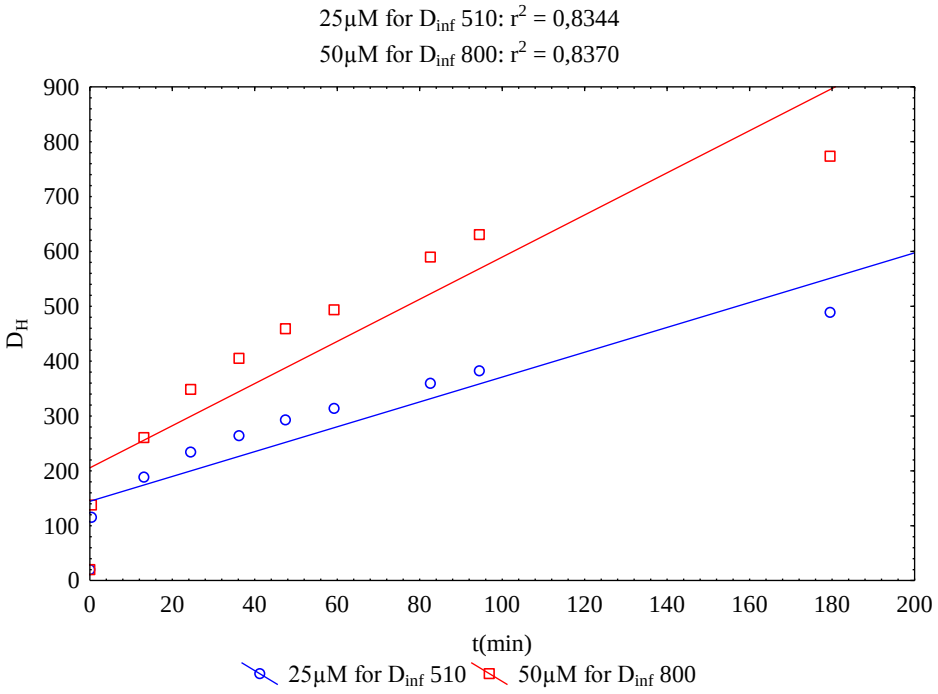

Figure 11 - 2D scatterplots of D_H (nm) versus t at D_0 20 (nm) in relation to different concentrations c of 25 µm of D_{inf} 510 and 50 µm of D_{inf} 800

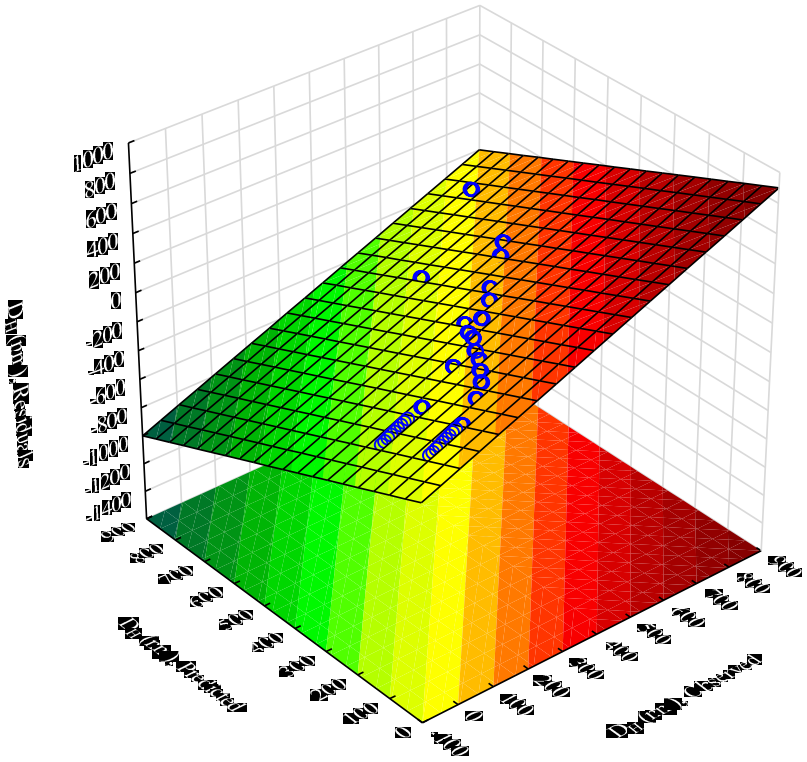

Figure 12 - Dependent variable D_H (nm) observed versus predicted versus residuals

3.4 Testing possible application of special versions of Novotny generalized isotherms for fitting time-dependent changes of agglomeration of nanoparticles

3.4.1 Background of the study

One of the most interesting results of the nanoparticle research is its success in the accumulation of findings from various disciplines and their rapid application in practice. Recent observations (although in the meantime based on limited data) revealed that agglomeration kinetics, which is closely connected with their respective toxicity, comprises some useful similarities to the electrosorption of species like sodium thiosulfate. In the past, the study of interactions of thiosulfate ions on charged surfaces was usually associated with their voltammetric determination on the surface of polarized electrodes. Collection of more data and findings on the electrosorption accumulation of the thiosulfate on the electrode could be utilized, for example, in "cathodic stripping voltammetry" (CSV) for its determination. This effect takes place

in the potentiostatically initiated electrosorption of thiosulfate and the formation of products of $Hg_2S_2O_3$ at a surface of a mercury electrode[66]. On the other hand, the application of a cathodic potential scan resulted in a reduction of Hg_2^{2+} to Hg. Therefore, CSV-signal of thiosulfate is useful for its analytical determination. Direct indicative of electrocapillary measurements[10,32] proved an adsorption of thiosulfate at potentials more positive than –0.35 V versus (SCE).

More accurate measurements and theoretical considerations[14,67,68] led to the model's relationships which captured much better the complex of present interactions between the particle and the charged interface as well as particle-particle interactions, including the formation of agglomerates of nano dimensions. One of the most up-to-date researches is the study of the formation and behaviour of nano-particles, for example, nanosilver particles[34]. Significant toxic effects of the size of silver nanoparticles have been proved recently. It comprises research on their growth kinetics, dependence on time, concentration and experimental conditions. An essential part of this study is to search for sensitive and effective ways of data fitting and evaluation. In practice, for the growth of the observed agglomerates, the model kinetics of the first order is applied. Such a simple model which is used in a wide-ranging of monitored transformable variables provides only average values of the kinetic parameters. For instance, it does not distinguish the initial formation of the initial aggregates from their next steady growth, hence the application of the present particle-particle and other interactions. Therefore, the study on the adsorption/electro-sorption processes and more or less closer analogies between adsorption and aggregation improved the possibilities of fitting and evaluating (nano) particle agglomeration.

3.4.2 Results and discussion

On the basis of the previously published findings associated with the study of the conditions of determining thiosulfate ions by using adsorptive voltammetry techniques, it can be assumed that for a polarized mercury electrode at potentials around −0.1 V against the saturated calomel electrode (SCE), specific interactions between the thiosulfate and the electrode surface[10,32] occurred producing $Hg_2(S_2O_3)$.

The extent of this effect would have grown fairly well with potentials *E* more positive than –0.1 V versus (SCE). The results indicated the presence of strong particle-particle interactions in the adsorbed Hg_2 (S_2O_3)-layer. At a constant potential of –0.1 V therefore, using the above-mentioned electrocapillary CCDT technique, a dependence of interfacial tension γ versus the logarithm of the concentration *log c* of the thiosulfate ions was obtained.

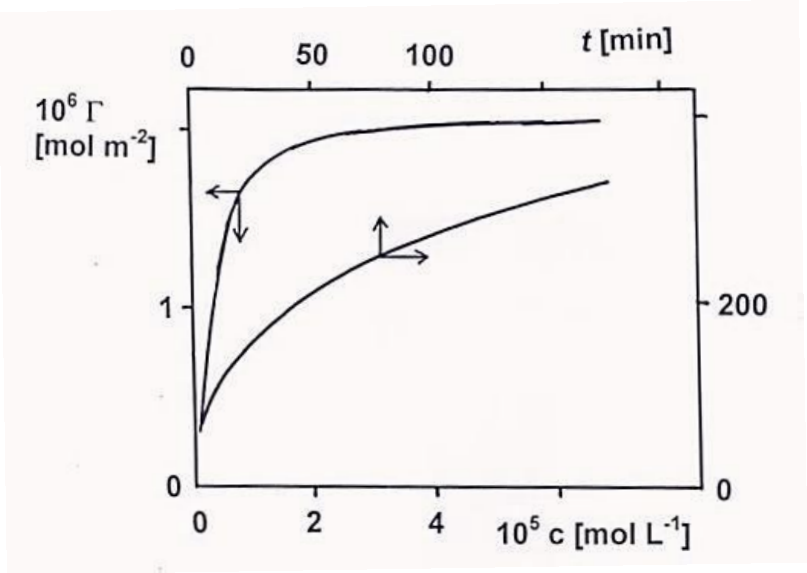

Figure 13 - Adsorption isotherm Γ versus concentration *c* of the thiosulfate; time-dependent changes of diameter *D* of nAg

From the Gibbs-Lippmann equation (Eq. 10)[10,32], the corresponding adsorption isotherm Γ of the thiosulfate, i.e. the dependence of its surface concentration Γ on the volume concentrations *c* (Figure 13) was calculated as follows:

$$d\gamma = -qdE - \Gamma d\mu, \; and \;\; \Gamma = -(d\gamma/d\mu)_E \qquad \text{Eq. 10}$$

where γ, *q*, *E*, Γ and μ denote the interfacial tension, surface charge density, potential, surface concentration (excess) of the adsorbate and the chemical potential, respectively. Under increasing *c*, the Γ versus *c* dependence approached its maximum (limit) value Γ_{max}. Eq. 10 can be used to determine the dependence of the relative surface coverage $\theta = \Gamma / \Gamma_{max}$ versus *c*. Using the recent findings, it can be[9,10,67] expressed (or fitted) mathematically, for example, by the model relationship (Eq. 11) as follows:

$$\frac{\theta}{1-\theta} exp(-\sum_{1=0}^{n} A_i \theta^i) = \beta\ c \quad \text{Eq. 11}$$

where A_i, i and β denote the coefficients, order of the polynomial term and interaction (adsorption) coefficient. Eq. 11, therefore, represents a special case of its more general form (Eq. 12)[9,10,67] as follows:

$$f_1(Y) exp[f_2(Y)] = kx\ or\ f(X,Y) \quad \text{Eq. 12}$$

which generally include the functions of (relative) magnitudes defined as the independent (X) and dependent (Y) variables in the following way (Eq. 13):

$$X = \frac{x-x_0}{x_m-x_0}\ or\ (x-x_0)\ or\ \frac{x}{x_m};\ Y = \frac{y-y_0}{y_m-y_0}\ or\ \frac{y}{y_m} \quad \text{Eq. 13}$$

where x, y, X, Y denote the general or relative magnitudes and x_0, y_0, x_m, y_m are the parameters. The logarithmic and modified equation (Eq. 11)[9,10,67] resulted in Eq. 14 as follows:

$$Z = ln\frac{\theta}{(1-\theta)c} = \sum_{i=0}^{n} A_i \theta^i = A_0 + A_1\theta + A_2\theta^2 + \cdots \quad \text{Eq. 14}$$

Analogously[9,10,67], the description of the agglomeration process of nanoparticles can also comprise the formation of the initial aggregates and subsequent growth of nano- or micro-particles (undergoing a transport mechanism). For silver nanoparticles, it was schematically illustrated by the hydrodynamic diameters D versus t dependence (see Figure 8 above). Its fitting, based on Eqs. 11 to 14 can be applied, as well as, producing the size of the initial diameter D_0 and the parameters of $D=D(t)$. As shown in Figures 14 and 15, Eqs. 15 and 16 can be used to estimate the value of D_0~50 nm corresponding to the best linearity of Z versus Y in the range of Y from 0.1 to 0.4, and to provide optimum fitting of Y versus t (Figure 16).

$$Z = ln\frac{Y}{(1-Y)t} = \sum_{i=0}^{n} A_i Y^i, n = 2 \quad \text{Eq. 15}$$

$$Y = \frac{\Delta D}{\Delta D_m};\ \Delta D = D - D_0;\ \Delta D_m = D_m - D_0; x = t\ or\ \Delta t \quad \text{Eq. 16}$$

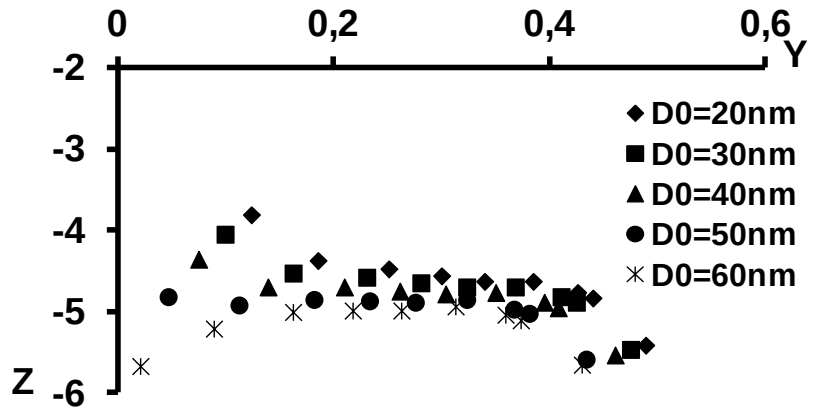

Figure 14 - Z versus *Y* plot at D_m = 400 nm and various values of D_0 (see Eq. 15)

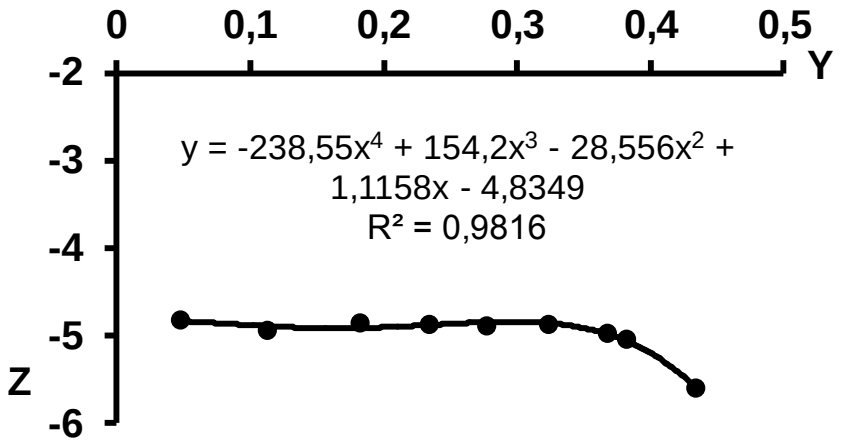

Figure 15 - Fitting *Z* versus *Y* following Eq. 15 at D_0=50 nm and D_m=400 nm

Based on the data for 10 μM Ag and for the above-estimated D_0 = 50 nm and D_m = 400 nm (see Figure 8) the dependencies $y = ln[(D_m–D)/(D_m–D_0)]$ versus $x = t$ could also be linearized as clearly as described in Eq. 17[34].

$$ln\frac{(D_m-D)}{(D_m-D_0)} = -kt \qquad \text{Eq. 17}$$

This linearization $y=k_1x+q$ in Excel provided the values of the parameters *k*, *q* and the correlation coefficient R^2 as shown in Figure 16.

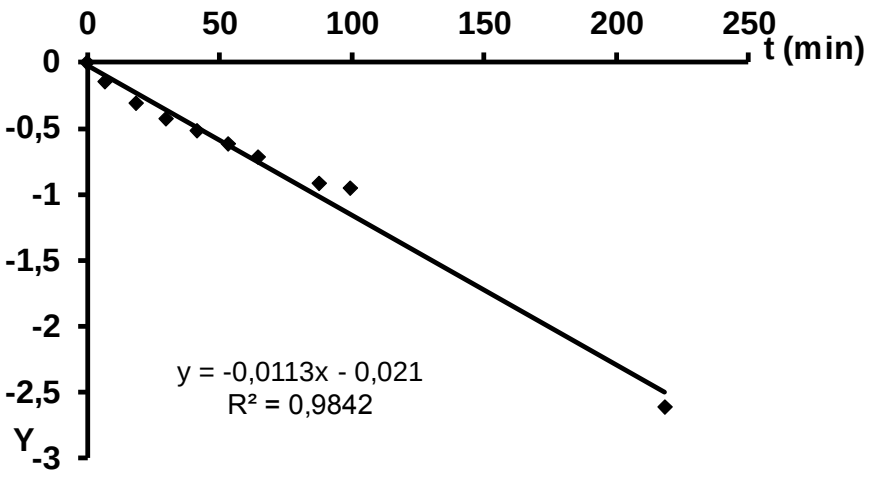

Figure 16 - Linearization $y=k_1x+q$ following Eq. 17; 10 μM Ag; D_0=50 nm; D_m=400 nm

Further, the linearization of the experimental data was repeated excluding the value of D_0 and starting with the first experimental value obtained for D_1 at t_1. The parameter values k_1, q, R^2 evaluated from Eq. 18 under steady growth conditions of nAg (excluding D_0) are plotted in Figure 17. For these purposes, Eq. 18 was utilized.

$$ln\frac{(\Delta D_m-\Delta D_i)}{(\Delta D_m-\Delta D_1)} = k_1(t_i - t_1) = k_1\Delta t \qquad \text{Eq. 18}$$

where $\Delta D_i=D_i-D_1$, $\Delta t=t_i-t_1$, $\Delta D_m=D_m-D_1$ are the differences in diameters, time and rate of diameters. From the experimental data, $y_i = ln[(\Delta D_m-\Delta D_i)/(\Delta D_m-\Delta D_1)]$ versus $x_i = t_i-t_1$ was subsequently determined. Dependencies of y_i versus x_i were linearly described at progressively different selected values ΔD_m, in the range of 320 nm to 400 nm. The results indicated that the best linearization was achieved at ΔD_m=360 nm. At this optimum value ΔD_m, a segmented linearization was then applied[14] on y_i versus x_i. The linearization dependencies (y_i versus x_i) were always selected from a group sets of five points: 1st set (x_i;y_i), i from 0 to 4; 2nd set (x_i; y_i), i from 1 to 5; 3rd set (x_i; y_i), i from 2 to 6; 4th set (x_i; y_i), i from 3 to 7; 5th set (x_i; y_i), i from 4 to 8. Results of the segmented linearization are shown in Figure 18.

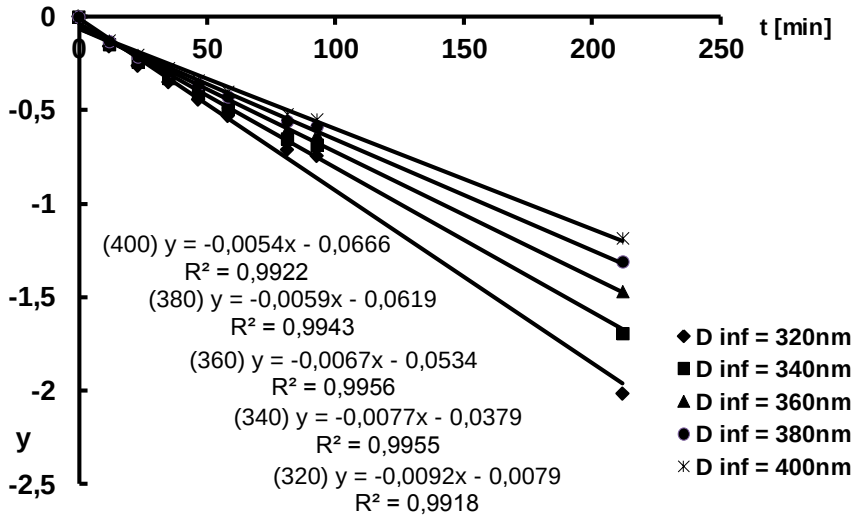

Figure 17 - Linearization of the sets of (x_i; y_i) data following Eq. 18; 10 μM Ag; ΔD_m between 320 nm and 400 nm

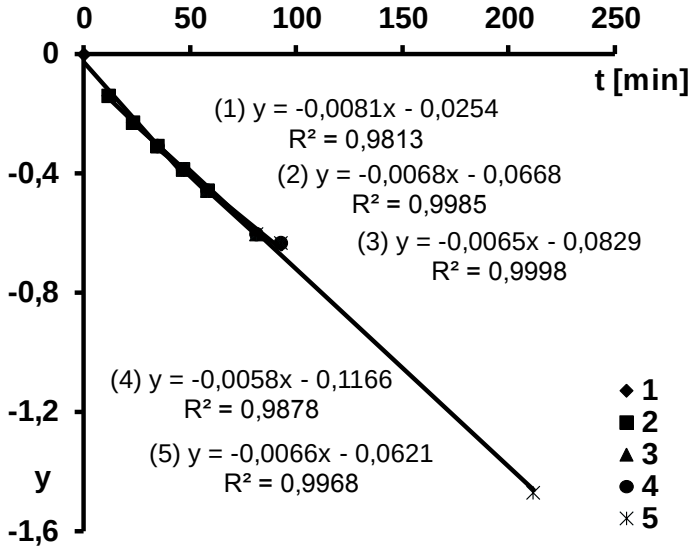

Figure 18 - Linearization of the sets of (x_i; y_i) data following Eq. 18; 10 μM Ag; ΔD_m= 360 nm

This implies that the time constants (by variable x) for the individual segments were not quite constant and were to some extent changing within the progress of agglomeration (also with *t*). This information was consistent with the assumption on the similarities between aggregation and adsorption processes discussed earlier.

4. CONCLUSIONS

4.1 Utilization of the potential response of the silver amalgam electrodes (AgAE) for assessing the process of ion exchange water treatment and pre-treatment

The study described the results of the changes in the Nernstian potentiometric behaviour of the silver electrode (AgE) and silver amalgam electrode (AgAE) for ion exchange water treatment including their pre-treatment. After the addition of $AgNO_3$ to the monitored sequence of water samples *Vi*, the diagrams of the *E* versus *Vi* for AgE and AgAE were measured and plotted. Unlike the AgE, AgAE provided acceptable reproducibility of results, useful for further research and practice, for example, in the field of water treatment monitoring.

4.2 Utilization of the potential signal of the silver amalgam electrodes (AgAE) for estimating changes in the concentration of an aqueous $ZnSO_4$ solution by nanofiltration

Basic potentiometric testing of sensitivity and behaviour of the advanced zinc amalgam electrode (ZnAE) in aqueous solutions of $ZnSO_4$ was reported. The calibrations of mixed potential *E* versus *log c* dependences were obtained. The reproducible linear concentration ranged from $2 \cdot 10^{-5}$ to $5 \cdot 10^{-2}$ $mol \cdot L^{-1}$. The zinc amalgam electrode (ZnAE) allowed sufficiently sensitive detection of concentration changes of $ZnSO_4$ (from 60 $mg \cdot L^{-1}$ to 2 $mg \cdot L^{-1}$) corresponding to the use of nanofiltration. Such potentiometric detection carried out in model solutions before and after the nanofiltration steps provided data that were in a reasonable agreement with the analysis of Zn using ICP-OES.

4.3 Characterization of the kinetics of silver particles agglomeration

The study on the analysis of the kinetics of particles growth of electrically charged silver nanoparticles or sub-microparticles of toxic concentrations between 25 and 50 μmol·L was investigated. The analysis and fitting time-dependences of the diameters *D* of the silver colloidal agglomerates employing atomic force microscopy and optical analytical techniques showed significant findings on the behaviour of the

silver nanoparticles or sub-microparticles concerning their growth kinetics, maximum diameters D_{inf} and the initial nanoparticlesdiameters D_0.

4.4 Verification of the possible application of special variants of Novotny generalized isotherm for fitting time changes of the agglomeration of nanoscale particles

The assessment of the agglomeration kinetics of waste nanoparticles based on its partial similarities to the electrosorption processes was discussed. In the case of the agglomeration of silver nanoparticles and the electrosorption of the sodium thiosulfate on the mercury polarized electrode at –0.1 V versus (SCE), specified useful similarities between both types of the processes were presented and applied. Alternative possibilities of fitting and evaluating some kinetic average parameters of aggregation utilizing the recently proposed relationships and isotherms were described.

4.5 Determined regression equations for the dependent variables y and D_H

Regression equations were described for the responses y and D_H in relation to *t*, D_0 and *c* respectively. The models were statistically significant ($p < 0.05$) or (F-value > p-value) with high values of the coefficient of determination (R^2) between 91 and 99 %. It is recommended that replications of the experimental data would be necessary to confirm the present findings established herein.

5. LITERATURE

1. COMNINELLIS, C., CHEN, G. *Electrochemistry for the Environment*. Springer, New York: 2010, 563 p. ISBN 978-0-387-36922-8.
2. KORYTA, J., DVOŘÁK, J. *Principles of Electrochemistry*. J. WILEY & SONS, New York: 1987.
3. SCHOLZ, F. *Electroanalytical Methods*, Springer-Verlag, Berlin: 2002.
4. NOVOTNÝ, L. *Obecná a aplikovaná elektrochemie pro životní prostředí*. Výukové materiály. ÚEnviChI, FCHT, Univerzita Pardubice: 2017.
5. GHERASIM, C. V., HANCKOVÁ, K., PALARČÍK, J., MIKULÁŠEK, P. *J. Membr. Sci.* 2015, 490, 9(15), 46-56. ISSN: 0376-7388.
6. GHERASIM, C. V., MIKULÁŠEK, P. *Desalination* 2014, 343, 67-74. ISSN: 0011-9164.
7. HÜBNER, P. *Úprava vody v energetice.* Praha: Vydavatelství VŠCHT, 2010. ISBN 978-80-7080-746-0.
8. PITTER, P. *Hydrochemie*. 3. dopl. vyd. Praha: Vydavatelství VŠCHT, 1999. 568 s. ISBN 80-03-00525-62.
9. NOVOTNÝ, L. Proceedings: (ŠTULÍK, K., KALVODA, R. Editors). *Electrochemistry for Environmental protection*. UNESCO-ROSTE, Venice: 1996, p. 49-87.
10. NOVOTNÝ, L. Prague, 1998. 695 s. Dr.Sc. Thesis. Acad. Sci. of the Czech Republic.
11. NOVOTNÝ, L., YOSYPCHUK, B. *Chem. Listy* 2000, 94(12), 1118-1120.
12. YOSYPCHUK, B., NOVOTNÝ, L. *Rev. Anal. Chem.* 2002 32, 141-151.
13. ŠELEŠOVSKÁ, R. Pardubice, 2015. Habilitation thesis. Univerzita Pardubice.
14. NOVOTNÝ, L. Úřad průmyslového vlastnictví Praha, UV 2014-30527, 2014.
15. NOVOTNÝ, L. Úřad průmyslového vlastnictví Praha, UV 2007-19501, 2007.
16. NOVOTNÝ, L. Úřad průmyslového vlastnictví Praha, PV 2001-1, 2001.
17. NOVOTNÝ, L. Úřad průmyslového vlastnictví Praha, PVZ 2017-41111, 2018.
18. NOVOTNÝ, L. *ChemZi* 2017, 13(1), p. 204.
19. NOVOTNÝ, L., PETRÁŇKOVÁ, R. *Anal Lett*. 2016, 49(1), 161-168. ISSN: 0003-2719.

20. NOVOTNÝ, L., KABUTEY, A., PETRÁŇKOVÁ, R., LANGÁŠEK, P. Změny nernstovského potenciometrického chování stříbrné a stříbrné amalgámové elektrody během iontoměničových úprav vody. *WASTE FORUM* 2018, 2, 209-213, accepted. ISSN: 1804-0195.
21. NOVOTNÝ, L., KOČANOVÁ, V., KABUTEY, A., KARÁSKOVÁ, A., DUŠEK, L., PETRÁŇKOVÁ, R., MIKULÁŠEK, P. Potentiometric signal of the zinc amalgam electrode for the detection of concentration changes of zinc sulphate due to its nanofiltration, *WASTE FORUM* 2018, 2, 117-123, 2018, accepted. ISSN: 1804-0.
22. NOVOTNÝ, L., KABUTEY, A., HRDÁ, K. Tentative assessment of the agglomeration kinetics of waste nanoparticles based on its partial similarity to the electrosorption processes. *WASTE FORUM* 2018, 2, 124-131, accepted. ISSN: 1804-0195.
23. NOVOTNÝ, L., OPRŠAL, J., PETRÁŇKOVÁ, R., KABUTEY, A., POUZAR, M., LANGÁŠEK, P. *Anal. Lett.* 2016, 49(1), 152-160. Attainable: https://doi.org/10.1080/00032719.2015.1045587.
24. NOVOTNY, L. *Book of Abstracts of the 15th International Conference on Electroanalysis*, (2014a), Malmo, Sweden, June 11-15, 2014, 189.
25. NOVOTNY, L. *Chem. Listy*. 2014b, 108: 777.
26. NOVOTNÝ, L. US Patent 5,173,101, 1992.
27. NOVOTNÝ, L. US Patent 5,294,324, 1994.
28. NOVOTNÝ, L. *Chem. Listy* 2001, 95, 147.
29. NOVOTNÝ, L. *XXIX. Moderní elektrochemické metody*, Jetřichovice, 25.5.-29.5.2009, Sborník přednášek (BAREK, J., NAVRÁTIL, T., Editors.), s. 82.
30. NOVOTNÝ, L. *Electroanalysis* 2000, 12, 1240.
31. FRARÈS, N. B., TAHA, S., DORANGE, G. *Desalination* 2005, 185, 245.
32. KRISTA, J., KOPANICA, M., NOVOTNY, L. *Anal. Chim. Acta* 1999, 386, 221.
33. NOVOTNÝ, L. *Fresenius J. Anal. Chem*. 1998, 342, 184.
34. OPRŠAL, J., KNOTEK, P., POUZAR, M., PALARČÍK, J., NOVOTNÝ, L. *Chem. Listy* 2013, 107, 386-392. ISSN 0009-2770.

35. BAREK, J., FISCHER, J., NAVRÁTIL, T., PECKOVÁ, K., YOSYPCHUK, B., ZIMA, J. *Electroanalysis* 2007, 19, 2003.
36. YOSYPCHUK, B., BAREK, J. *Crit. Rev. Anal. Chem*. 2009, 39, 189.
37. DANHEL, A., YOSYPCHUK, B., VYSKOČIL, V., ZIMA, J., BAREK, J. *J. Electroanal. Chem*. 2011, 656, 218.
38. STAHLBUSH, J. R., STROM, R. M. *React. Polym*. 1990, 13, 233.
39. DE DARDEL, F., ARDEN, T. V. *Ion Exchangers*, Wiley-VCH verlag GmbH & Co. KGaA, 2008.
40. JELÍNEK, L. a kol. *Desalinační a separační metody v úpravě vody*. 1. vyd., VŠCHT, Praha 2009.
41. SCHÄFER, A. I., FANE, A. G., WAITE, T. D. *Nanofiltration – Principles and Applications*. Elsevier Ltd., Oxford, UK p 147, 2005.
42. SHAHEEN, S. M., EISSA, F. I., GHANEMB, K. M., GAMAL EL-DINC, H. M., AL ANANYB, F. S. *J. Environ Manage* 2013, 128, 514.
43. VILA, M., SANCHEZ-SALCEDO, S., CICUENDEZ, M., IZQUIERDO-BARBA, I., VALLET-REGI, M. *J. Hazard Mater* 2011, 192, 71.
44. Agency for Toxic Substances and Disease Registry (ATSDR), Regulations and Advisories - Regulations and Guidelines Applicable to Zinc and Zinc Compounds, 2003, http://www.atsdr.cdc.gov/toxprofiles/tp60-c8.pdf.
45. Government Order of the Czech Republic No. 61 of January 29th, 2003. On the indicators and values of permissible pollution of surface water and wastewater, mandatory elements of the permits for discharge of wastewater into surface water and into sewerage systems, and on sensitive areas.
46. CHOO, K. H., KWON, D. J., LEE, K. W., CHOI, S. *J. Environ Sci. Technol*. 2002, 36, 1330.
47. BOURANENE, S., FIEVET, P., SZYMCZYK, A., EL-HADISAMER, M., VODONNE, A. *J. Membr. Sci*. 2008, 325, 150.
48. GONZÁLEZ-MUÑOZ, M. J., RODRÍGUEZ, M. A., LUQUE, S., ÁLVAREZ, J. R. *Desalination* 2006, 200, 742.
49. BELKHOUCHE, N. E., DIDI, M. A., TAHA, S., FARÈS, N. B. *Desalination* 2009, 239, 58.

50. BORBÉLY, G., NAGY, E. *Desalination* 2009, 240, 218.
51. NOVOTNÝ, L., KOČANOVÁ, V., LANGÁŠEK, P., PETRÁŇKOVÁ, R. *XXXV. Modern Electrochemical Methods*, Jetřichovice, 18-22 May 2015, Proceedings (BEST Servis Ústí nad Labem, eds.), p. 108.
52. MONTASER, A., GOLIGHTLY, D. W. *Inductively coupled plasmas in analytical atomic spectrometry*, 3rd edition, VCH Publisher, Inc, New York 1992.
53. WELZ, B., SPERLING, M. *Atomic absorption spectrometry*, 3rd edition, Verlag Chemie, Weinham:1999.
54. WIJNHOVEN, S. W. P., PEIJNENBURG, J. G. M., HERBERTS, C. A., HAGENS, W. I., OOMEN, A. G., HEUGENS, E. H. W., ROSZEK, B. *Nanotoxicology* 2009, 3: 109-138. doi:10.1080/17435390902725914.
55. LEE, S. M., SONG, K. C., LEE, B. S. *Korean Journal of Chemical Engineering* 2010, 27: 688-692. doi:10.1007/s11814-010-0067-0.
56. NOWACK, B., KRUG, H. F., HEIGHT, M. *Environmental Science & Technology* 2011, 45: 1177–1183. doi:10.1021/es200435m.
57. RIBEIRO, F., GALLEGO-URREA, J. A., JURKSCHAT, K., CROSSLEY, A., HASSELLOV, M., TAYLOR, C., SOARES, A. M. V. M., LOUREIRO, S. *Science of the Total Environment* 2014, 466-467: 232-241. doi:10.1016/j.scitotenv.2013.06.101.
58. POLASKOVA, P., NOVOTNY, L., OSTATNA, V., PALECEK, E. *Electroanalysis* 2009, 21: 625-630. doi:10.1002/elan.200804459.
59. VESELA, H., SUCMAN, E. *Acta Veterinaria Brno* 2013a, 82: 203–208. doi:10.2754/avb201382020203.
60. VESELA, H., SUCMAN, E. *Czech Journal of Food Science* 2013b, 31:401-06.
61. HEYROVSKÝ, J., KŮTA, J. *Principles of polarography*, Publishing House of the Czech Acad. Sci, Prague 1965.
62. OBERDORSTER, E. *Environmental Health Perspectives* 2004, 112: 1058. doi:10.1289/ehp.7021.

63. ROMER, I., WHITE, T. A., BAALOUSHA, M., CHIPMAN, J. K., VIANT, M. R., LEAD, J. R. *Journal of Chromatography A.* 2011, 1218: 4226-4233. doi:10.1016/j.chroma.2011.03.034.
64. KABUTEY, A. *Statistical Analysis of Multivariate Data – Exercises*. Pardubice, 2016. 130 pages. University of Pardubice, Faculty of Chemical Technology, Institute of Environmental and Chemical Engineering. Guarantor: prof. RNDr. Milan Meloun, Dr.Sc.
65. Statsoft, 2013. Inc. Tulsa, OK74104, USA.
66. CIGLENECKI, I., COSOVIC, B. *Electroanalysis* 1997, *9*, 775.
67. NOVOTNÝ, L. *69. Zjazd chemikov, Vysoké Tatry 11-15 September 2017*, (ChemZi 13/1, Slovenská chemická spoločnosť, ed.), str. 203, 2017.
68. NOVOTNÝ, L. *XXXVI. Modern Electrochemical Methods,* Jetřichovice, 23-27 May 2016, Proceedings (BEST Servis Ústí n. L, ed.), p. 152.
69. BANDŽUCHOVA, L., ŠELEŠOVSKA, R., NAVRATIL, T., CHYLKOVA, J. *Electroanalysis* 2013, 25: 213-222. doi:10.1002/elan.201200365.
70. FADRNA, R., CAHOVA-KUCHARIKOVA, K., HAVRAN, L., YOSYPCHUK, B., FOJTA, M. *Electroanalysis* 2005, 17: 452-59. doi:10.1002/elan.200403181.
71. NAVRATIL, T., BAREK, J. *Critical Reviews in Analytical Chemistry* 2009, 39:131-147. doi:10.1080/10408340903011796.
72. SELESOVSKA, R., BANDZUCHOVA, L., NAVRATIL, T., CHYLKOVA, J. *Electrochimica Acta* 2012, 60: 375-383. doi:10.1016/j.electacta.2011.11.071.
73. YOSYPCHUK, B., BAREK, J. *Critical Reviews in Analytical Chemistry* 2009, 39:189–203. doi:10.1002/chin.200944275.

6. PUBLICATION ACTIVITIES

6.1 Papers

1. NOVOTNÝ, L., OPRŠAL, J., PETRÁŇKOVÁ, R., KABUTEY, A., POUZAR, M., LANGÁŠEK, P. *Anal. Lett.* 2016, 49(1), 152-160. Attainable: https://doi.org/10.1080/00032719.2015.1045587.
2. NOVOTNÝ, L., KABUTEY, A., PETRÁŇKOVÁ, R., LANGÁŠEK, P. Změny nernstovského potenciometrického chování stříbrné a stříbrné amalgámové elektrody během iontoměničových úprav vody. *WASTE FORUM* 2018, 2, 209-213, accepted. ISSN: 1804-0195.
3. NOVOTNÝ, L., KABUTEY, A., HRDÁ, K. Tentative assessment of the agglomeration kinetics of waste nanoparticles based on its partial similarity to the electrosorption processes. *WASTE FORUM* 2018, 2, 124-131, accepted. ISSN: 1804-0195.
4. NOVOTNÝ, L., KOČANOVÁ, V., KABUTEY, A., KARÁSKOVÁ, A., DUŠEK, L., PETRÁŇKOVÁ, R., MIKULÁŠEK, P. Potentiometric signal of the zinc amalgam electrode for the detection of concentration changes of zinc sulphate due to its nanofiltration, *WASTE FORUM* 2018, 2, 117-123, 2018, accepted. ISSN: 1804-0.

6.2 Oral presentations

5. KABUTEY, A., NOVOTNÝ, L., PETRÁŇKOVÁ, R. Application of potentiometric analytical technique for heavy metals determination. *E.I.D.S. Summer Workshop,* Aveiro, Portugal, 26.4.-2.5.2015.
6. KABUTEY, A., NOVOTNÝ, L., PETRÁŇKOVÁ, R., KOČANOVÁ, V., WALLACE, E. *Proc. of the 3rd Int. Conf. Chem. Technol.* 1st ed. Prague (KALENDA, P., LUBOJACKÝ, J. Editors). Czech Society of Industrial Chemistry, 2015, Annex. ISBN: 978-80-86238-79-1.

6.3 Proceedings of conferences, posters

7. NOVOTNÝ, L., DUŠEK, L., VYSTRČILOVÁ, B., PETRÁŇKOVÁ, R., KABUTEY, A. *Chem. Listy* 2012, 106, 601, ISSN 1213-7103.

8. NOVOTNÝ, L., PETRÁŇKOVÁ, R., KABUTEY, A. *ChemZi* 2013, 9(1), 231. ISSN 1336-7242.
9. NOVOTNÝ, L., PETRÁŇKOVÁ, R., OPRŠAL, J., KABUTEY, A., POUZAR, M. *13th Workshop of physical chemists and electrochemists: sborník příspěvků 29.-30.5.2013*. Brno: Masarykova univerzita, 2013, p. 156-157. ISBN 978-80-7375-757-1.
10. NOVOTNÝ, L., LANGÁŠEK, P., PETRÁŇKOVÁ, R., KABUTEY, A. *Chem. Listy* 2014, 108(8), 795. ISSN 0009-2770.
11. NOVOTNÝ, L., PETRÁŇKOVÁ, R., OPRŠAL, J., KABUTEY, A., POUZAR, M. *Proc. of the 15th Int. Conf.* Malmö, 2014 (ESEAC, eds.), p. 199.
12. NOVOTNÝ, L., PETRÁŇKOVÁ, R., KABUTEY, A. *Sborník přednášek XXXIV. Moderní Elektrochemické Metody*. 2014 (BEST Servis Ústí n. L., ed.), s. 118-120. ISBN 978-80-905221-2-1.
13. NOVOTNÝ, L., LANGÁŠEK, P., PETRÁŇKOVÁ, R., KOČANOVÁ, V., KABUTEY, A., DUŠEK, L. *ChemZi* 2015, 11(1), 170. ISSN 1336-7242.
14. KABUTEY, A, NOVOTNÝ, L., KOČANOVÁ, V., PETRÁŇKOVÁ, R., LANGÁŠEK, P., WALLACE, E., DUŠEK, L. *ChemZi* 2015, 11(1), 170. ISSN 1336-7242.
15. NOVOTNÝ, L., KOČANOVÁ, V., DUŠEK, L., KABUTEY, A., PETRÁŇKOVÁ, R., KARÁSKOVÁ, A. *Sborník přednášek XXXVI. Moderní Elektrochemické Metody*. 2016, p. 155-157, ISBN 978-80-905221-4-5.
16. NOVOTNÝ, L., KOČANOVÁ, V., KABUTEY, A., DUŠEK, L. *Sborník příspěvků 68. sjezd chemiků*. Praha, 2016, p. 191, 1P-14. ISSN 2336-7202.
17. NOVOTNÝ, L., KOČANOVÁ, V., DUŠEK, L., KABUTEY, A., MIKULÁŠEK, P., PETRÁŇKOVÁ, R., KARÁSKOVÁ, A. *ChemZi* 2017, 13(1), p. 203.
18. NOVOTNÝ, L., KARÁSKOVÁ, A., KABUTEY, A., PETRÁŇKOVÁ, R. *Sborník přednášek XXXVIII. Moderní Elektrochemické Metody*. 2018 (BEST Servis Ústí n. L. ed.), p. 183-186, ISBN 978-80-905221-6-9.
19. NOVOTNÝ, L., KOČANOVÁ, V., KABUTEY, A., KARÁSKOVÁ, A., DUŠEK, L., PETRÁŇKOVÁ, R., MIKULÁŠEK, P. *Proc. of the 17th Int. Conf.* Rhodes, 2018 (ESEAC, eds.), p. 159.

20. NOVOTNÝ, L., KABUTEY, A., KARÁSKOVÁ, A., KOČANOVÁ, V., MIKULÁŠEK, P. *Proc. of the 17th Int. Conf.* Rhodes, 2018 (ESEAC, eds.), p. 224.

6.4 Seminar/Symposium

21. Eastern Analytical Symposium, 18.11.-20.11.2013, New Jersey, USA.
22. Scientific Writing and Academic Conference, University of Pardubice, 24.11.-25.11.2014, Pardubice, Czech Republic.